ISSN 1063-7850, Technical Physics Letters, 2012, Vol. 38, No. 5, pp. 456–459. © Pleiades Publishing, Ltd., 2012.
Original Russian Text © Ya.Ya. Kudryk, A.V. Zinovchuk, 2012, published in Pis'ma v Zhurnal Tekhnicheskoi Fiziki, 2012, Vol. 38, No. 10, pp. 14–20.

The Effect of Current Crowding on the Internal Quantum Efficiency of InAsSb/InAs Light-Emitting Diodes

Ya. Ya. Kudryk and A. V. Zinovchuk*

Lashkarev Institute of Semiconductor Physics, National Academy of Sciences of Ukraine, 03025 Kiev, Ukraine
Ivan Franko Zhytomyr State University, 10008 Zhytomyr, Ukraine
**e-mail: zinovchuk@zu.edu.ua*

Received January 11, 2012

Abstract—The effect of current crowding on the internal quantum efficiency (IQE) of InAsSb/InAs light-emitting diodes (LEDs) operating in the middle-infrared (mid-IR) range ($\lambda = 3$–$5\ \mu$m) has been studied. Calculations based on a modified model of recombination coefficients show that current crowding leads to a significant decrease in the IQE of LEDs, which is especially pronounced in longer-wavelength devices (23% at $\lambda = 3.4\ \mu$m versus 39% at $\lambda = 4.2\ \mu$m). The obtained results indicate that the effect of current crowding should be taken into consideration as an additional nonthermal mechanism of IQE decrease in mid-IR LEDs.

DOI: 10.1134/S1063785012050252

A general problem for light-emitting diodes (LEDs) operating in various spectral intervals is related to the phenomenon of "crowding" of the current lines in some regions of a multilayer LED structure, which is caused by rather high resistivities of layers and specific features of the LED exterior design that are determined by the need to extract radiation. The current crowding effect is well known in LEDs operating in both visible (based on InGaN [1] and AlGaInP [2]) and IR (InAsSb [3]) spectral intervals. Several investigations have been devoted to numerical simulation [4, 5] and analytical modeling [1, 6, 7] of current spreading in LEDs. These works were aimed at improvement of current spreading in the active region of devices through optimization of the internal parameters (resistance and thickness of the substrate, confinement layers, and current-spreading layers) and the geometry of contacts. It was also pointed out that current crowding led to the activation of nonradiative recombination, local heating of the device structure, and a resulting decrease in the IQE of LEDs. However, no quantitative calculations of the influence of current crowding on the IQE have been performed so far.

Because of the dominant role of nonradiative recombination in narrow-bandgap semiconductors, the current crowding effect must be especially pronounced in LEDs operating in the mid-IR range. For this reason, we have studied mid-IR LEDs based on InAsSb/InAs heterostructures, the production technology and main performance parameters of which are well known (see, e.g., [8, 9]). This Letter presents the results of calculations of the IQE of InAsSb/InAs LEDs as a function of the injection level with allowance for the current crowding effect.

We have considered InAsSb/InAs LEDs of standard planar design with a round n-contact of radius $r_0 = 50\ \mu$m on the upper surface (Fig. 1a). The spatial distributions of current density were performed by assuming axial symmetry of the structure (LEDs have a cylindrical shape with external radius $R = 300\ \mu$m). Taking into account data [8] on the internal structure of InAsSb/InAs LEDs, the proposed model takes into account the three most important layers, which are characterized by their thicknesses and resistivities: p-InAs substrate (d_p, ρ_π), n-InAsSb active layer (d_{al}, ρ_{al}), and upper n-InAsSbP spreading layer (d_n, ρ_n). Calculations were performed for the following numerical values of these parameters:

$$d_n = 5\ \mu\text{m}, \quad \rho_n = 6.2 \times 10^{-4}\ \Omega\ \text{cm};$$

$$d_p = 200\ \mu\text{m}, \quad \rho_p = 4.1 \times 10^{-2}\ \Omega\ \text{cm}; \text{ and } d_{al} = 2\ \mu\text{m}.$$

It is assumed that the active layer is characterized by a nonlinear resistance of the p–n junction, which is calculated using the diode current–voltage characteristic as follows:

$$\rho_{al} = \varphi_{al}/(d_{al} j_0(\exp(e\varphi_{al}/\beta kT) - 1)),$$

where φ_{al} is the voltage drop on the active layer, k is the Boltzmann constant, T is the absolute temperature, e is the electron charge, β is the ideality factor of the p–n junction, and j_0 is the saturation current density. All calculations were performed for $\beta = 1$, $T = 300$ K, and the saturation current density j_0 determined by the Shockley formula derived in the theory of the ideal p–n junction [10].

As is known, it is possible to control the LED wavelength within the mid-IR spectral range by varying the concentration of Sb in the active layer. In the present

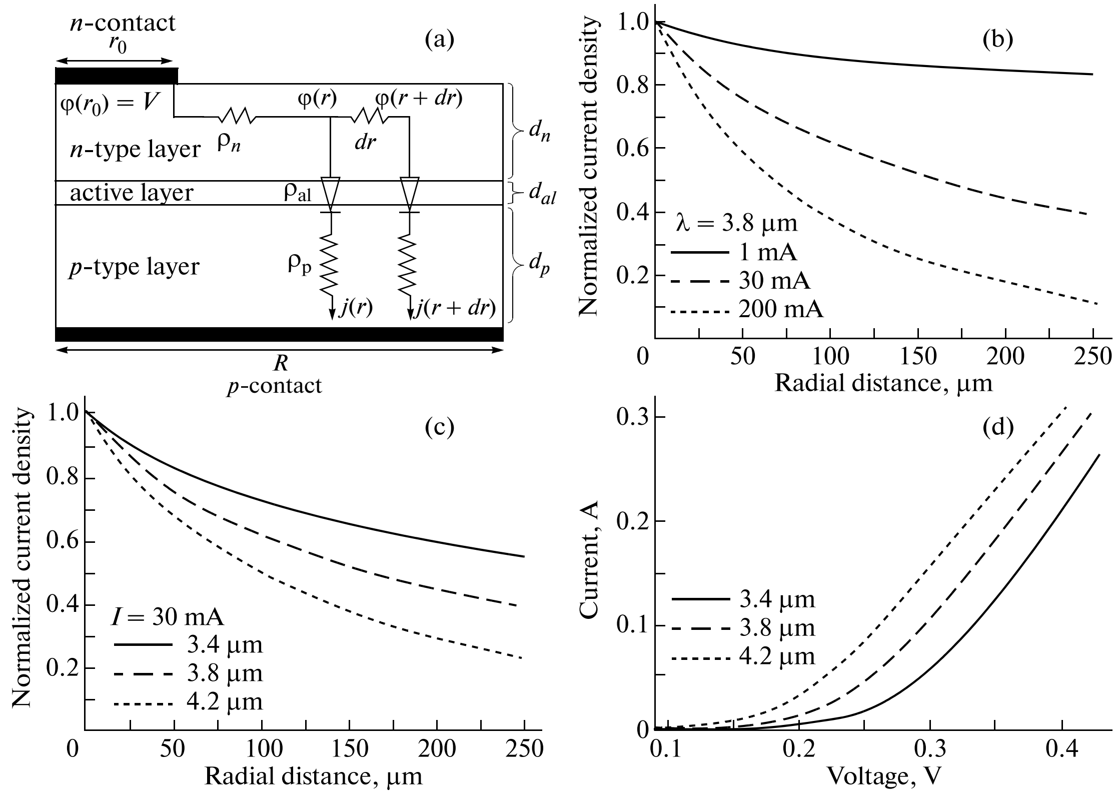

Fig. 1. Planar InAsSb LED: (a) transverse cross section and equivalent circuit scheme; (b, c) plots of the normalized current density vs. radial coordinate (measured from the n-contact edge) in LEDs operating (b) at $\lambda = 3.8$ μm and various injection levels and (c) at $I = 30$ mA and various emission wavelengths; (d) current–voltage characteristics calculated with allowance for the current crowding in LEDs at various emission wavelengths.

work, we have studied LEDs emitting at three practically important wavelengths $\lambda = 3.4$, 3.8, and 4.2 μm. The only difference between the models of LEDs for these wavelengths was the saturation current density j_0, which depended on the bandgap width (E_g) in the n-InAsSb active layer as $j_0 \sim \exp(-E_g/kT)$.

By applying the Kirchhoff laws to the equivalent scheme of LED (Fig. 1a), it is possible to show that the electric potential φ in the upper n-type layer depends on the radial coordinate (r) according to the following equation:

$$\frac{d^2\varphi(r)}{dr^2} + \frac{1}{r}\frac{d\varphi(r)}{dr} = \frac{\rho_n}{d_n}j(r), \qquad (1)$$

where $j(r)$ is the vertical component of the current density. Assuming that the p-contact potential is zero ($\varphi_p = 0$), the potential drop between the upper n-contact and the lower p-contact can be expressed as follows:

$$\varphi(r) = (\rho_p d_p + \rho_{al} d_{al}) j(r). \qquad (2)$$

In order to obtain an analytical solution to system of equations (1), (2), we have assumed that the potential drop on the active layer is independent of the radial coordinate r and is determined by the difference between the applied bias voltage V and the potential drop on the p-type layer:

$$\varphi_{al} = V - I(\rho_p d_p)/S,$$

where I is the total current and S is the light-emitting area. Under the above assumptions, a solution to system of equations (1), (2) with respect to the current density for the given physical conditions can be written as follows:

$$j(r) = \frac{VK_0(\alpha r)}{K_0(\alpha r_0)(\rho_p d_p + \rho_{al} d_{al})}, \qquad (3)$$

where $\alpha = \sqrt{\rho_n/(d_n(\rho_p d_p + \rho_{al} d_{al}))}$ and $K_0(\alpha r)$ is the modified zero-order Bessel function of the second kind. Formula (3) describes the dependence of the spreading current density on the distance from the upper n-contact edge. Assuming that the current density under the n-contact is $j(r_0)$ and integrating Eq. (3) over the entire LED area, we obtain the LED current–density characteristic with allowance for the current crowding (Fig. 1d). In addition, Figs. 1b and 1c show the radial profiles of the normalized current density in diodes operating at various injection levels and different emission wavelengths, respectively. As low levels of injection, the current crowding is negligibly small because of a rather large resistance of the active layer

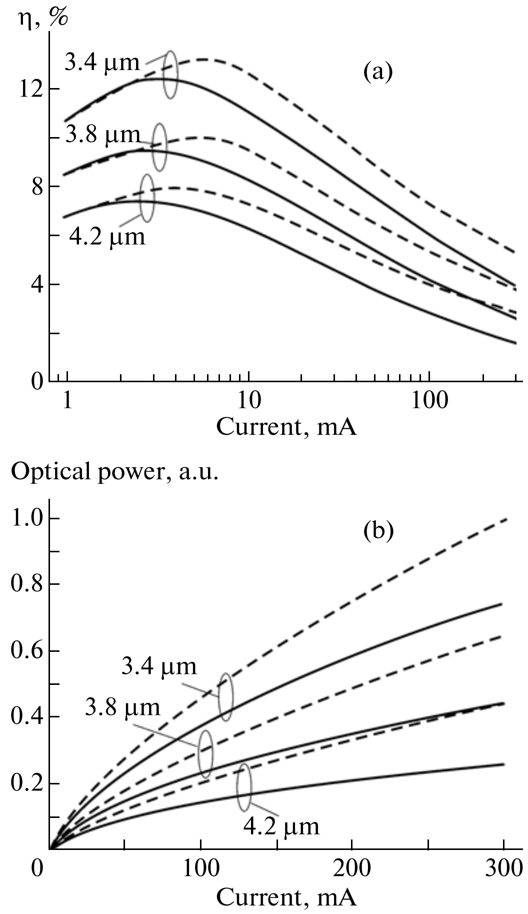

Fig. 2. Plots of (a) IQE η and (b) optical power vs. pumping current for InAsSb LEDs operating at various wavelengths calculated with (solid curves) and without (dashed carves) allowance for the current crowding.

(ρ_{al}) compared to that of the other layers. An increase in the level of injection leads to a rapid decrease in ρ_{al} and the current crowding under the upper *n*-contact. The enhanced current crowding with the increasing LED wavelength is explained by the dependence of ρ_{al} on the bandgap width E_g in the InAsSb active layer. For the same level of injection, ρ_{al} in long-wavelength LEDs is smaller and the current crowding is more pronounced.

According to the model of recombination coefficients, the current density in the active layer is related to the concentration of injected carriers *n* as follows:

$$j/(ed_{al}) = An + Bn^2 + Cn^3,$$

where *A, B*, and *C* are the coefficients of nonradiative (Shockley–Reed), radiative, and Auger recombination, respectively. Using this relation and Eq. (3), one can determine the radial profile $n(r)$ of the concentration of injected carriers. Finally, for the known $n(r)$ function, the IQE of LEDs under consideration can be calculated as follows:

$$\eta = \frac{P/h\nu}{I/e} = \frac{d_{al}2\pi\int_0^R Bn^2(r)rdr}{I/e}, \quad (4)$$

where $P/h\nu$ is the number of photons emitted from the active layer per second, *P* is the optical power, $h\nu$ is the photon energy, and I/e is the number of electrons injected into the active layer per second.

Figure 2 compares the results of calculations of the IQE (η) and optical power of InAsSb LEDs operating at various wavelengths as functions of the pumping current. In these calculations, the value of coefficient *A* was assumed to be the same for all LEDs ($A = 1.0 \times 10^6$ s^{-1}), while coefficients *B* and *C* were determined by the following formulas [11, 12]:

$$B = 3.0 \times 10^{-10}(E_g/1.5)^2(\text{cm}^3/\text{s})$$

$$C = 1.2 \times 10^{-27}E_g^{-5/2}\exp(-4.25E_g)(\text{cm}^6/\text{s}),$$

where E_g [eV] is the bandgap width in the active layer. Dashed curves in Fig. 2 represent the IQE calculated without allowance for the current crowding (with *j* and *n* assumed to be spatially independent). At low injection levels ($I < 3$ mA), the calculations performed both with and without allowance for the current crowding give virtually the same η values (solid and dashed curves in Fig. 2 coincide). However, at high injection levels, the phenomenon of current crowding leads to a significant decrease in the IQE.

As can be seen from Fig. 1b, the current density under the upper *n*-contact can significantly exceed the average value. For example, at $I = 200$ mA, the maximum current density reaches $j_{max} = 220$ A/cm^2, whereas the average value is $j_{av} = 72$ A/cm^2. This leads to the intensification of Auger recombination under the upper *n*-contact with the resulting decrease in the IQE. Because of a stronger current crowding in longer-wavelength LEDs, a decrease in the IQE in this case is especially significant. For example, at $I = 200$ mA, the IQE decrease caused by the current crowding in a 3.4-μm LED is about 23%, while, in an otherwise identical 4.2-μm LED operating at the same current, the IQE drops by 39%.

In conclusion, we have quantitatively estimated the effect of current crowding on the IQE of InAsSb/InAs LEDs operating in the mid-IR range. The obtained results indicate that the effect of current crowding at high injection levels decreases the IQE by more than 20%. All calculations were performed with self-heating being neglected, which allows the effect of current crowding to be considered as an additional nonthermal mechanism of IQE decrease in mid-IR LEDs. In contrast to the temperature factor, which can be partly eliminated in a pulsed pumping regime, the effect of current crowding must be taken into account in the development of new IR LEDs operating in both pulsed and steady-state loading regimes.

REFERENCES

1. X. Guo and E. F. Schubert, J. Appl. Phys. **90** (8), 4191 (2001).
2. R. M. Fletcher, C. P. Kuo, T. D. Osentowski, K. H. Huang, M. G. Craford, and V. M. Robbins, J. Electron. Mater. **20** (12), 1125 (1991).
3. V. K. Malyutenko, O. Yu. Malyutenko, A. D. Podoltsev, I. N. Kucheryavaya, M. A. Remennyi, and N. M. Stus, Appl. Phys. Lett. **79** (25), 4228 (2001).
4. V. K. Malyutenko, A. V. Zinovchuk, and O. Yu. Malyutenko, Semicond. Sci. Technol. **23**, 085004 (2008).
5. I. Yu. Evstratov, V. F. Mymrin, S. Yu. Karpov, and Yu. N. Makarov, Phys. Status Solidi (c) **3** (6), 1645 (2006).
6. W. B. Joyce and S. H. Wemple, J. Appl. Phys. **41** (9), 3818 (1970).
7. R. M. Perks, A. Porch, D. V. Morgan, and J. Kettle, J. Appl. Phys. **100** (8), 083109 (2006).
8. N. V. Zotova, S. S. Kizhaev, S. S. Molchanov, T. I. Molchanova, T. S. Lagunova, B. V. Pushnyi, and Yu. P. Yakovlev, Semiconductors **37**, 955 (2003).
9. B. Matveev, N. Zotova, S. Karandashov, M. Remennyi, N. Il'inskaya, N. Stus, V. Shustov, G. Talalakin, and J. Malinen, Proc. IEEE Proc. Optoelectron. **145** (5), 254 (1998).
10. W. Shockley, Bell Syst. Tech. J. **28** (3), 435 (1949).
11. D. Z. Garbuzov, J. Lumin. **27** (1), 109 (1982).
12. B. L. Gel'mont and Z. N. Sokolova, Sov. Phys. Semicond. **16**, 1067 (1982).

Translated by P. Pozdeev